AIP Journal of Applied Physics

Growth of -FeSi 2 films via noble-gas ion-beam mixing of Fe/Si bilayers

M. Milosavljevi, S. Dhar, P. Schaaf, N. Bibi, Y-L. Huang, M. Seibt, and K. P. Lieb

Citation: Journal of Applied Physics **90**, 4474 (2001); doi: 10.1063/1.1405818
View online: http://dx.doi.org/10.1063/1.1405818
View Table of Contents: http://scitation.aip.org/content/aip/journal/jap/90/9?ver=pdfcov
Published by the AIP Publishing

Articles you may be interested in

Investigation of microstructure and soft magnetic properties of Fe 65 Co 35 thin films deposited on different underlayers
J. Appl. Phys. **107**, 09A325 (2010); 10.1063/1.3356228

Enhanced interface mixing of Fe Si bilayers on preamorphized silicon substrates
Appl. Phys. Lett. **90**, 051901 (2007); 10.1063/1.2432952

Preparation and structural investigation of epitaxially grown antiferromagnetic FeSn 2 (001) thin films on InSb(001)
J. Appl. Phys. **94**, 3573 (2003); 10.1063/1.1595144

Mössbauer study of the magnetism and structure of amorphous and nanocrystalline Fe 81x Ni x Zr 7 B 12 (x=10–40) alloys
J. Appl. Phys. **94**, 638 (2003); 10.1063/1.1578701

Ion beam mixing of ZnO/SiO 2 and Sb/Ni/Si interfaces under swift heavy ion irradiation
J. Appl. Phys. **91**, 1129 (2002); 10.1063/1.1425439

Re-register for Table of Content Alerts

Create a profile.

Sign up today!

[This article is copyrighted as indicated in the article. Reuse of AIP content is subject to the terms at: http://scitation.aip.org/termsconditions. Downloaded to] IP: 131.227.68.227 On: Wed, 30 Apr 2014 17:13:22

JOURNAL OF APPLIED PHYSICS VOLUME 90, NUMBER 9 1 NOVEMBER 2001

Growth of β-$FeSi_2$ films via noble-gas ion-beam mixing of Fe/Si bilayers

M. Milosavljević
II. Physikalisches Institut, Universität Göttingen, Bunsenstrasse 7-9, D-37073 Göttingen, Germany and VINČA Institute of Nuclear Sciences, PO Box 522, 11001 Belgrade, Yugoslavia

S. Dhar and P. Schaaf[a)]
II. Physikalisches Institut, Universität Göttingen, Bunsenstrasse 7-9, D-37073 Göttingen, Germany

N. Bibić
II. Physikalisches Institut, Universität Göttingen, Bunsenstrasse 7-9, D-37073 Göttingen, Germany and VINČA Institute of Nuclear Sciences, PO Box 522, 11001 Belgrade, Yugoslavia

Y-L. Huang and M. Seibt
IV. Physikalisches Institut, Universität Göttingen, Bunsenstrasse 13-15, D-37073 Göttingen, Germany

K. P. Lieb
II. Physikalisches Institut, Universität Göttingen, Bunsenstrasse 7-9, D-37073 Göttingen, Germany

(Received 27 December 2000; accepted for publication 29 July 2001)

A detailed study of the formation of β-$FeSi_2$ films by ion-beam mixing of Fe/Si bilayers with noble gas ions is presented. Fe films of 35–50 nm deposited on Si (100) were irradiated with 80–700 keV Ar, Kr, or Xe ions in a wide temperature interval, from room temperature to 600 °C. The structures were analyzed by Rutherford backscattering spectroscopy, x-ray diffraction, conversion electron Mössbauer spectroscopy, elastic recoil detection analysis, cross-section high resolution transmission electron microscopy, and energy dispersive x-ray spectroscopy. Already after Xe irradiation at 300 °C the whole Fe layer is transformed to a mixture of Fe_3Si, ε-FeSi, and β-$FeSi_2$ phases. At 400–450 °C, a unique, layer by layer growth of β-$FeSi_2$ starting from the surface was found. A full transformation of 35 nm Fe on Si to a 105 nm β-$FeSi_2$ layer was achieved by irradiation with 205 keV Xe to 2×10^{16} ions/cm^2, at a temperature of 600 °C. The fully ion-beam grown layers exhibit a pronounced surface roughness, but a sharp interface to Si. This structure is assigned to a growth of β-$FeSi_2$ grains in a local surrounding of interdiffused silicon. Rapid diffusion of silicon to the surface was observed during all ion irradiations. Single-phase β-$FeSi_2$ layers were also synthesized by vacuum annealing for 2 h at 600 °C of 35 nm Fe/Si bilayers premixed with Xe at 450 °C. In this case, the layers form with a smoother surface topography. It is concluded that ion-beam mixing can be used successfully for growth of β-$FeSi_2$ layers at moderate temperatures, either directly or combined with postirradiation annealing. *© 2001 American Institute of Physics.*
[DOI: 10.1063/1.1405818]

I. INTRODUCTION

In recent years there has been an increasing effort in the development of new silicon-based optoelectronic materials because of their possible implementation in integrated opto- and micro-electronic devices.[1] One such material is β-$FeSi_2$, a novel direct band gap semiconductor,[2–4] with $E_g = 0.85-0.87$ eV, which matches the wavelength of 1.5 μm of silica optical fibers, thus making it suitable for optoelectronic communications. Furthermore, this material has other favorable characteristics, such as high photoabsorption and thermoelectric coefficients, good stability at high temperatures, corrosion resistivity, and high abundance of its nontoxic constituents Fe and Si. This opens new fields of wide applications,[4–6] e.g., for high efficiency solar cells, photodetectors, and thermoelectric devices.

In a solid-state reaction, iron and silicon can form various solutions and compounds that have different allotropic phases and can coexist. Therefore growth of a particular phase requires special processing techniques. The low temperature phases are Fe_3Si and FeSi, the latter starting to grow at 450–500 °C.[7,8] Iron-disilicide forms in a cubic, metastable γ-$FeSi_2$ phase, a stable orthorhombic β-$FeSi_2$ phase, and at temperatures above 930 °C in a stable tetragonal α-$FeSi_2$ phase. Both α and γ phases have metallic properties. The semiconducting β-$FeSi_2$ phase starts to nucleate from FeSi at about 550 °C,[7] but for complete growth of a β-$FeSi_2$ layer much higher temperatures are needed. Various techniques have been investigated for the fabrication of β-$FeSi_2$ layers, such as solid phase epitaxy,[7–9] codeposition of Fe and Si,[9] molecular beam epitaxy,[5,10] ion-beam synthesis,[3,4] ion-beam assisted deposition,[11] or pulsed laser deposition.[12] However, all these processing methods require extended high temperature treatments, at 800–900 °C, for the formation and/or stabilization of the β-$FeSi_2$ structure. A lower growth tempera-

[a)]Corresponding author; electronic mail: pschaaf@uni-goettingen.de

 © 2001 American Institute of Physics

[This article is copyrighted as indicated in the article. Reuse of AIP content is subject to the terms at: http://scitation.aip.org/termsconditions. Downloaded to] IP: 131.227.68.227 On: Wed, 30 Apr 2014 17:13:22

ture of β-$FeSi_2$ layers was achieved by using an interposed Ni layer between Fe and Si in solid phase epitaxy,[13] or by reactive deposition epitaxy of very thin layers in ultrahigh vacuum conditions.[14] Synthesis of α, β, and γ-$FeSi_2$ precipitates, at 320 °C, was reported in ion-beam induced epitaxial crystallization (IBIEC) of Si (100), preimplanted with Fe.[15,16] Ion-beam mixing of predeposited Fe layers on a Si substrate appears to be another route to synthesize β-$FeSi_2$ layers, where energetic ions can supply additional energy to the matrix and reduce the temperature required for full growth. In addition, the required irradiation fluence can be significantly lower than that used for direct ion-beam synthesis. So far, only a few studies of the formation of Fe-silicides by ion-beam mixing have been reported,[17–19] in which the growth of β-$FeSi_2$ was detected to set in already at temperatures of 220–400 °C, although this phase was found in a mixed structure with pure Fe and other Fe-silicides. Full formation of β-$FeSi_2$ layers by ion-beam mixing of Fe/Si structures has just recently been reported.[20]

In this article we present a detailed study of the possibilities of applying ion-beam mixing with noble-gas ions to achieve full growth of β-$FeSi_2$ layers on Si at moderate temperatures. We have investigated the influence of the main parameters (ion species, fluence, energy, target temperature, and Fe film thickness) on the formation of the β-$FeSi_2$ phase. The Fe/Si bilayers were irradiated with Xe, Kr, and Ar ions in a wide temperature range, from room temperature (RT) to 600 °C. Complete characterization of the stoichiometry, phases, and microstructure of the intermixed layers was carried out. The results obtained are compared to those reported for thermal growth of the β-$FeSi_2$, and the particular influence of ion irradiation is discussed.

II. EXPERIMENTAL PROCEDURE

Iron layers were deposited by electron-beam evaporation on lightly doped *n*-type Si (100) wafers at the TESLA facility in the Vinča Institute.[21] Before being mounted in the chamber, the substrates were cleaned by a standard procedure, a rinse in diluted HF and in deionized H_2O. Prior to deposition they were sputter cleaned with a high intensity 1.5 keV Ar ion beam. The Fe layers were grown to a thickness of 35 and 50 nm, at a rate of 0.5 nm/s. The pressure in the chamber during deposition was maintained at 1×10^{-6} mbar.

Noble-gas ion irradiation and ion-beam analyses[22] of the samples were performed at the IONAS implanter in Göttingen.[23] We used Xe, Kr, and Ar ions to irradiate a series of samples at temperatures ranging from RT to 600 °C. For most implantations the energy was chosen to adjust the projected ion range R_p at about 20 nm behind the original Fe/Si interface. These values are 250 and 350 keV for Xe, 175 and 250 keV for Kr, and 80 and 120 keV for Ar, for the 35 and 50 nm Fe/Si bilayers, respectively. To investigate the effect of ion energy, an additional series of 35 nm Fe/Si samples was irradiated with 150–700 keV Xe ions. A sample area of 1×1 cm^2 was implanted homogeneously to fluences ranging from 5×10^{15} to 4×10^{16} ions/cm^2 at a beam current of 2.5 $\mu A/cm^2$. The target heater was designed to allow fast heating and cooling of the targets, while additional heating induced by the ion beam can be neglected at elevated temperatures. The pressure in the implantation chamber was in the low 10^{-7} mbar region. Isochronal postirradiation annealing of selected samples was performed in a vacuum furnace at 600 °C at a pressure of 10^{-6} mbar.

Rutherford backscattering spectroscopy (RBS) was performed with 900 keV He^{2+} ions, using two Si surface barrier detectors positioned at a scattering angle of 165°. Random spectra were taken at near-normal incidence, and the experimental data were analyzed with the RUMP[24] code. All samples were analyzed by x-ray diffraction (XRD), at 5° incidence, using Cu $K\alpha$ emission. Phase analyses were also performed at room temperature by conversion electron Mössbauer spectroscopy (CEMS) with a ^{57}Co/Rh source and constant acceleration drive, detecting the conversion electrons emitted from the upper 150 nm of the sample.[25] Isomer shifts are given relative to α-Fe, which was also used for velocity calibration. A least-squares fit routine by superimposing Lorentzian lines was used for the analysis of the spectra.[26] Selected samples were analyzed by elastic recoil detection analysis (ERDA), using the time-of-flight equipment at the Accelerator Laboratory of the University of Helsinki and a 53 MeV $^{127}I^{10+}$ beam.[27] Microstructural characterization was performed by high resolution cross-sectional transmission electron microscopy (TEM) and energy dispersive x-ray spectroscopy (EDXS).

III. RESULTS

A. Treatment of 50 nm Fe/Si bilayers

The results of RBS analyses of 50 nm Fe/Si samples, irradiated with 350 keV Xe, 250 keV Kr, and 120 keV Ar ions are shown in Fig. 1. Experimental spectra are presented in the left column, and the deduced depth profiles of the components are given in the right column. It can be seen that in all irradiated samples the initially isolated Fe and Si layers (a) become fully intermixed. The shape of the depth profiles inferred that Fe-silicides are formed. In the sample implanted with Xe, to 2×10^{16} ions/cm^2 at 450 °C (b), the components have uniform concentration profiles with the atomic ratio of Fe/Si=43(3)/57(3). When the irradiation temperature is raised to 550 °C we observe an increased diffusion of silicon to the surface, which results in lowering and broadening of the Fe depth profile, but also in a broader silicide/silicon interface. In the sample implanted to 4×10^{16} Xe ions/cm^2 (c), the concentration ratio at the surface is Fe/Si=37(3)/63(3), and towards the interface with the Si substrate the ratio is Fe/Si=33(3)/67(3). Irradiation at the sample temperature with 2×10^{16} Kr ions/cm^2 (d) yields a constant atomic ratio of Fe/Si=41(3)/59(3), and with 4×10^{16} Ar ions/cm^2 (e) the Fe/Si atomic ratio is nearly the same but there is also more silicon diffused to the surface.

The results of XRD analyses are presented in Fig. 2. The as-deposited sample (a) shows only a broad peak of nonreacted iron. In the irradiated samples all elemental iron is consumed by the growth of the stable FeSi and β-$FeSi_2$ phases. The intensities of the diffraction peaks suggest that these two phases have about equal fractions in the sample implanted at 450 °C (b), while in those implanted at 550 °C

[This article is copyrighted as indicated in the article. Reuse of AIP content is subject to the terms at: http://scitation.aip.org/termsconditions. Downloaded to] IP: 131.227.68.227 On: Wed, 30 Apr 2014 17:13:22

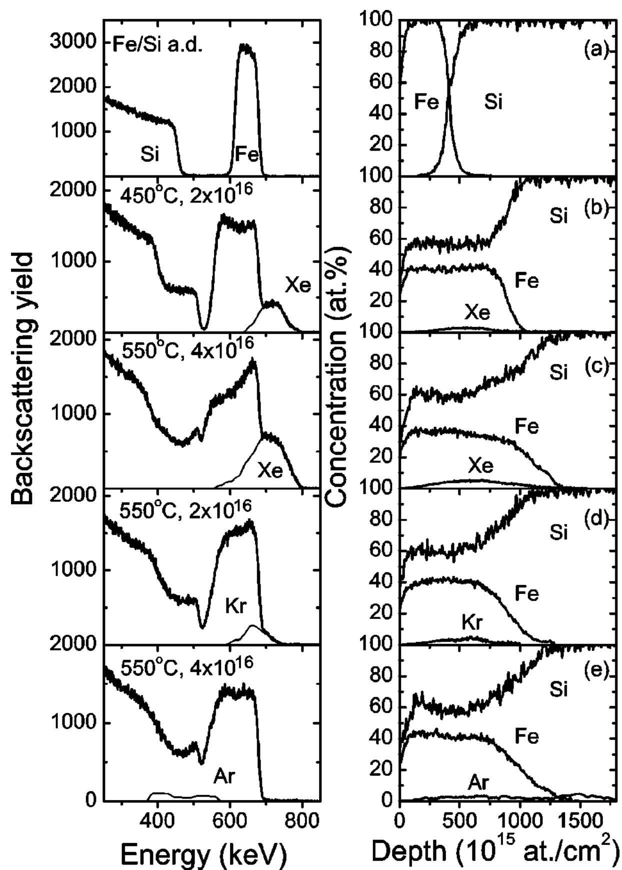

FIG. 1. RBS spectra and the deduced depth profiles of 50 nm Fe/Si: (a) as-deposited and (b)–(e) irradiated with 350 keV Xe, 250 keV Kr, and 120 keV Ar. The irradiation temperature and the ion fluence are indicated in the figure.

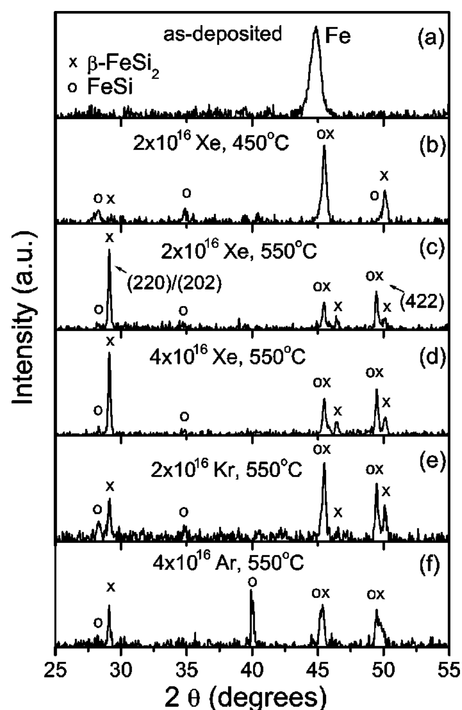

FIG. 2. XRD analysis of 50 nm Fe/Si samples: (a) as deposited and (b)–(f) samples irradiated with 350 keV Xe, 250 keV Kr, and 120 keV Ar.

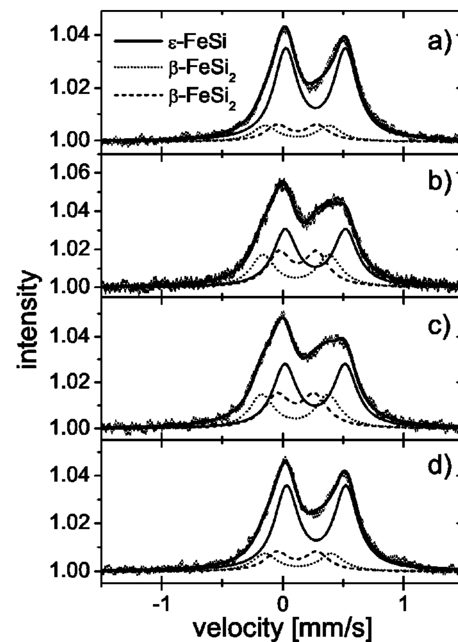

FIG. 3. CEMS spectra and analysis of 50 nm Fe/Si samples irradiated with: (a) 350 keV Xe, 2×10^{16} 1/cm^2, 450 °C; (b) 350 keVXe, 4×10^{16} 1/cm^2, 550 °C; (c)250 keV Kr, 2×10^{16} 1/cm^2, 550 °C; and (d) 120 keV Ar, 4×10^{16} 1/cm^2, 550 °C.

the β-$FeSi_2$ phase dominates. However, for the reflections at 2θ between 45° to 46° and 49° to 50° there is an overlap of signals, due to which it is difficult to distinguish between the two phases in this region. As we are reaching the concentration ratio of Fe/Si≈1/2, samples implanted at 550 °C to 2×10^{16} and 4×10^{16} Xe ions/cm^2 [(c) and (d)], the most intensive diffraction peaks are from (220)/(202) and (422) β-$FeSi_2$. Irradiation with Kr (e) and Ar (f) ions does not yield as intense reflections from these β-$FeSi_2$ planes.

The fractions of the Fe-silicide phases were determined by CEMS analysis, which also confirmed that no nonreacted elemental Fe remained in the irradiated samples. They consist of the nonmagnetic phases ε-FeSi and β-$FeSi_2$, as shown in Fig. 3. The spectra were fitted with two doublets corresponding to the two nonequivalent Fe sites in β-$FeSi_2$ having the hyperfine parameters Fe-I: $\delta=0.09(2)$ mm/s, $\Delta=0.54(2)$ mm/s; Fe-II: $\delta=0.10(2)$ mm/s, $\Delta=0.323(2)$ mm/s), and an additional doublet that corresponds to ε-FeSi [$\delta=0.27(2)$ and $\Delta=0.49(2)$]. No signs for texture effects could be observed in the Mössbauer spectra. The given values coincide with those reported in the literature,[15,28–35] where Desimoni and Sanchez gave a nice overview about the parameters.[30] While the hyperfine parameters of the ε-FeSi phase have been widely accepted,[31–34] there was a discrepancy in those of the β-$FeSi_2$ phase. Only the work by Fanciulli, Weyer, and coworkers[28,29] solved the problem, cleverly employing epitaxial films and texture analyses, which were later confirmed by measurements on single crystals.[33] These experiments finally clarified the hyperfine parameters of the latter phase. The values obtained in the present analyses coincide nicely with this improved model for the β-$FeSi_2$. Only the values for the quadrupole splittings of the two subspectra of this phase are slightly increased to 0.33(2) and 0.54(2) mm/s, still

[This article is copyrighted as indicated in the article. Reuse of AIP content is subject to the terms at: http://scitation.aip.org/termsconditions. Downloaded to] IP: 131.227.68.227 On: Wed, 30 Apr 2014 17:13:22

agreeing with the given values [0.315(8) mm/s and 0.525(8) mm/s] of Fanciulli *et al.*[28,29] within our error limits. This slight increase might be due to stresses and the polycrystallinity (nanocrystallinity) of the films in contrast to the epitaxial samples or single crystals measured in the abovementioned references. When trying to include some fraction of α-$FeSi_2$ into the analysis,[32–35] the quality of the fits worsened. Nevertheless, in these samples, some minor contributions (<5%) of the latter cannot be excluded from the Mössbauer spectra alone. The fraction ratio of the two β-$FeSi_2$ sites does not deviate from 1:1 within the experimental error [always better than 1:1.08(9)].

In the sample implanted at 450 °C with 2×10^{16} Xe ions/cm^2 (a), the phase concentration is 87(7)% FeSi and 13(7)% β-$FeSi_2$. These phase fractions agree well with the constant Fe/Si atomic ratio deduced by RBS analysis, suggesting that the two phases might be distributed homogeneously throughout the silicide layer. The sample implanted at 550 °C with 4×10^{16} Xe ions/cm^2 (b) consists of 46(2)% FeSi and 54(2)% β-$FeSi_2$. Here the depth profiles resolved by RBS are not constant, meaning that the β-$FeSi_2$ phase has probably grown more towards the inner regions of the mixed layer. A homogeneous phase distribution that matches the Fe/Si atomic ratio deduced from RBS, of 48(3)% FeSi and 52(3)% β-$FeSi_2$, is also observed in the sample implanted at 550 °C with 250 keV Kr to 2×10^{16} ions/cm^2 [Fig. 3(c)]. Irradiation with 120 keV Ar, to a higher fluence of 4×10^{16} ions/cm^2 (d), yields fractions of 71(5)% FeSi and only 29(5)% of β-$FeSi_2$. Considering the RBS profiles, it can be concluded that in this case the silicide layer is enriched with nonreacted Si, especially at the surface.

Because in the 50 nm Fe/Si layers we did not achieve full growth of β-$FeSi_2$, even at the relatively high Xe fluence of 4×10^{16} ions/cm^2, our further investigations focused on 35 nm Fe/Si samples.

B. Treatment of 35 nm Fe/Si bilayers

The initial energy for irradiation of 35 nm Fe/Si bilayers was again chosen to adjust the projected ion range at about 20 nm behind the Fe/Si interface. Here we focused on the influence of the processing parameters, mainly the target temperature, ion mass, fluence, and energy on the growth of the β-$FeSi_2$ phase.

1. Target temperature

A series of depth profiles, deduced from RBS spectra, of 35 nm Fe/Si samples implanted with 250 keV Xe, at temperatures from 300 to 600 °C, are illustrated in Fig. 4. The analysis confirms that ion irradiation induces a progressed Fe–Si intermixing and a solid state reaction of the components when increasing the target temperature. In the sample implanted at RT (not shown in the figure), the Fe and Si signals exhibit nonuniform, diffusion-like, depth profiles of the components within the intermixed region. Irradiation at 300 °C to 1×10^{16} Xe ions/cm^2 (b), induces full intermixing of the components, with Si moving to the surface, but the Fe and Si concentration profiles do not yet show regions with a constant Fe/Si atomic ratio. Ion implantation to the same fluence at 400 °C (c) results in homogeneous Fe and Si concentration profiles with the atomic ratio of Fe/Si=44(3)/56(3), which is in good agreement with the phase fractions measured by CEMS (see Table I). With increasing the ion fluence at this temperature, to 2×10^{16} ions/cm^2 (d), in the surface region the atomic ratio is Fe/Si=33(3)/67(3) and in the inner parts of the silicide Fe/Si=43(3)/57(3). After irradiation with 2×10^{16} Xe ions/cm^2 at 500 °C (e) we are close to the $FeSi_2$ stoichiometry, and actually for the fluence of 2×10^{16} Xe ions/cm^2 at 550 °C (f) the measured atomic ratio is Fe/Si=33(3)/67(3). At 600 °C uniform concentration profiles of Fe and Si are obtained at a lower Xe fluence, of 1×10^{16} ions/cm^2 (g), with Fe/Si=31(3)/69(3). Increasing the Xe fluence to 2×10^{16} ions/cm^2 at 600 °C (h) induces a further diffusion of silicon, which reaches a concentration of up to ~75 at. % at the surface. In Fig. 5 we present the depth

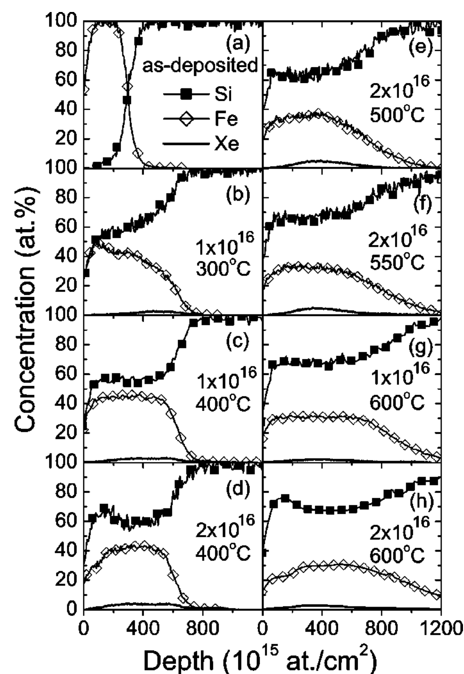

FIG. 4. RBS depth profiles of 35 nm Fe/Si samples: (a) as-deposited and (b)–(h) irradiated with 250 keV Xe ions at different temperatures and fluences.

TABLE I. Fe-silicide phase fractions formed by irradiation of 35 nm Fe/Si bilayers with 250 keV Xe, 175 keV Kr, and 80 keV Ar ions. Missing fraction is corresponding to magnetic phases.

Ion	Temperature (°C)	Fluence (ions/cm^2)	ϵ-FeSi (%)	β-$FeSi_2$ (%)
Xe	300	1×10^{16}	35(4)	30(4)
Xe	400	1×10^{16}	82(2)	18(2)
Xe	300	2×10^{16}	53(4)	47(4)
Xe	450	2×10^{16}	61(3)	39(3)
Xe	500	2×10^{16}	29(3)	71(3)
Xe	550	1×10^{16}	50(4)	50(4)
Xe	550	2×10^{16}	13(3)	87(3)
Xe	600	1×10^{16}	10(3)	90(3)
Xe	600	2×10^{16}	8(4)	92(4)
Kr	550	1×10^{16}	63(4)	37(4)
Kr	550	2×10^{16}	29(3)	71(3)
Ar	550	2×10^{16}	69(3)	31(3)

[This article is copyrighted as indicated in the article. Reuse of AIP content is subject to the terms at: http://scitation.aip.org/termsconditions. Downloaded to] IP: 131.227.68.227 On: Wed, 30 Apr 2014 17:13:22

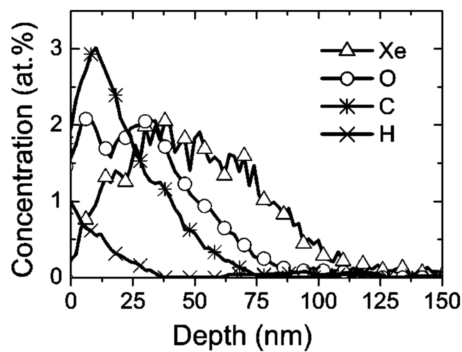

FIG. 5. ERDA depth profiles of Xe and reactive gas elements, in a 35 nm Fe/Si sample irradiated at 600 °C with 2×10^{16} Xe ions/cm^2.

profiles of Xe and of light elements for the latter sample, deduced by the highly sensitive ERDA technique. The implanted Xe is distributed within the silicide, reaching a concentration of up to 2 at. %. In the surface region we observe a contamination with up to 3 at. % of carbon and about 2 at. % of oxygen, which could not be determined by RBS. The depth profiles of Fe and Si resemble those obtained by RBS analysis. It should be noted that this sample has a portion of nonreacted silicon at the surface, which could adsorb contaminants when exposed to air.

Assuming that β-$FeSi_2$ layers are grown at 550–600 °C and using the bulk density of this phase (7.95×10^{22} atom/cm^3) in the RBS simulations, the calculated effective thickness of the grown layers is 95–105 nm. The combined interface and surface roughness deduced from RBS is rather large, which can be assigned to surface roughness, as will be seen from the TEM analysis. Hence the effective thickness was measured from the surface to the half-height of the Fe distribution towards silicon. The RBS spectra also reveal the XE profiles. They were compared with the results of TRIM calculations,[36] which give a projected range of $R_p=55$ nm and a width of $\Delta R_p=31$ nm [full width at half maximum (FWHM)], for 250 keV Xe implanted in 35 nm Fe on Si. In the sample implanted at RT, the maximum of the Xe distribution is positioned at 64(3) nm, i.e., behind the Fe/Si interface and within the Si substrate. The small difference compared to the TRIM results can be assigned to surface sputtering of Fe. When the target temperature is increased, the implanted Xe is distributed more towards the surface and the Fe sputtering is substantially lower, which is probably a consequence of a rapid change of the local atomic density at the surface. After irradiation at 450 °C we still register a double-peaked Xe concentration (see Fig. 13), one peak located within the silicide and the other at the silicide/silicon interface. At 500–600 °C the Xe distribution has only a single maximum, located within the silicide at a depth of 48(3) nm. In all irradiated samples the total amount of Xe agrees with that of the implanted fluence.

The XRD spectra of samples implanted at 250 keV, with 2×10^{16} Xe ions/cm^2 at 400–600 °C, are shown in Fig. 6. It can be seen that all iron has reacted in the formation of Fe-silicides. In samples implanted at 400 (a) and 450 °C (b), the dominating lines occur at 2θ between 45° to 46° and 49° to 50°, where the reflections from β-$FeSi_2$ and FeSi overlap.

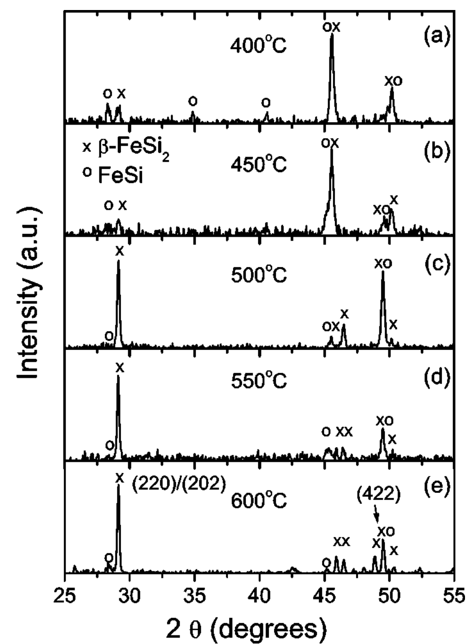

FIG. 6. XRD analysis of 35 nm Fe/Si samples implanted at 250 keV, with 2×10^{16} Xe ions/cm^2, at 400–600 °C (a)–(e).

As the irradiation temperature is raised there is an increased yield of the (220)/(202) and (422) β-$FeSi_2$ reflections. After irradiation at 500 °C the intensity of these reflections is nearly equal. A characteristic change of preferred orientation occurs between 500 (c) and 550 °C (d), leading to an increased yield of the (220)/(202) β-$FeSi_2$ reflections compared to (422). The samples implanted at 550 and 600 °C (e) exhibit a similar XRD spectra. However, in both spectra we still register small peaks in the angular regions where the diffraction lines from β-$FeSi_2$ and FeSi overlap.

The results of CEMS analyses of 35 nm Fe/Si irradiated with Xe, Kr, and Ar ions are summarized in Table I. After ion irradiation at RT (data not given in the table) the sample exhibits magnetic α-Fe and Fe_3Si phases. The sample implanted at 300 °C contains 31(4)% of the remaining Fe_3Si magnetic phase and of the paramagnetic ε-FeSi and β-$FeSi_2$ phases. All other samples contain only the paramagnetic phases. Already the irradiation at 300 °C produces a substantial amount of β-$FeSi_2$ whose fraction increases with the irradiation temperature, but after irradiation at 600 °C we still find 9(4)% of the monosilicide phase. Here the RBS and ERDA profiles indicate a silicon-rich $FeSi_2$ phase, and in the XRD analysis the FeSi content is at the detection limit. The fraction of the grown β-$FeSi_2$ phase as a function of irradiation temperature, for Xe fluence of 1×10^{16} ions/cm^2, is plotted in Fig. 7(a). It exhibits three distinct regions: from RT to 450 °C the β-$FeSi_2$ fraction gradually increases due to ion-beam mixing and tends to saturate at around 40%. From 450 to 500 °C the β-$FeSi_2$ content rapidly increases to about 90%. This can be assigned to thermal activation in the growth of FeSi and its rapid transformation to β-$FeSi_2$. For higher temperatures the β-$FeSi_2$ phase fraction saturates towards 100%.

[This article is copyrighted as indicated in the article. Reuse of AIP content is subject to the terms at: http://scitation.aip.org/termsconditions. Downloaded to] IP: 131.227.68.227 On: Wed, 30 Apr 2014 17:13:22

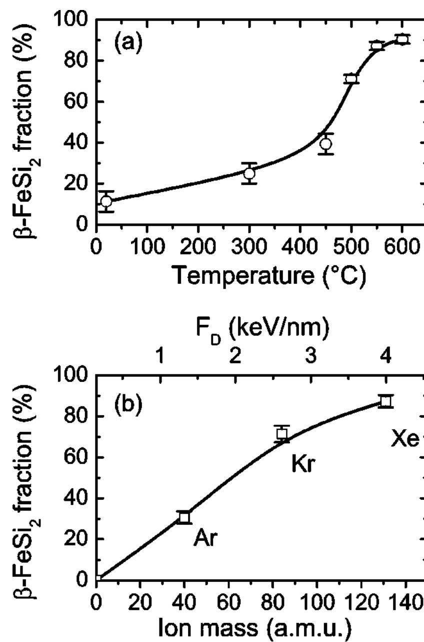

FIG. 7. Fraction of the grown β-$FeSi_2$ phase in 35 nm Fe/Si as a function of: (a) irradiation temperature for 250 keV Xe implated to 1×10^{16} Xe ions/cm^2 and (b) ion mass for 250 keV Xe, 175 keV Kr, and 80 keV Ar implated to 2×10^{16} Xe ions/cm^2.

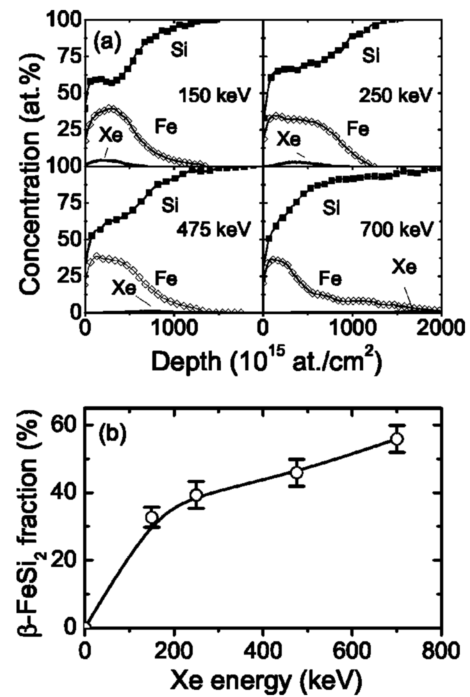

FIG. 8. RBS depth profiles (a) for 35 nm Fe/Si implanted with 150, 250, 475, and 700 keV Xe to 1×10^{16} Xe ions/cm^2 and (b) fraction of the β-$FeSi_2$ phase grown in these samples.

2. Ion species

Using the data from Table I, for Ar, Kr, and Xe implanted to 2×10^{16} ions/cm^2 at 550 °C, in Fig. 7(b) we have plotted the relative fraction of the grown β-$FeSi_2$ phase as a function of the ion mass. The maximum damage energy F_D, deposited within the silicide layer by Ar (1.3 keV/nm), Kr (2.8 keV/nm), and Xe (4.0 keV/nm) is also indicated in the figure. The less efficient formation of this phase with lighter Ar and Kr ions can be assigned to a lower deposited energy, as was also the case with 50 nm Fe/Si bilayers.

3. Ion energy

The analysis described so far proves that we are close to a full growth of the β-$FeSi_2$ phase by irradiation with Xe ions at 550–600 °C, but there is still a small fraction of FeSi even in the samples that have excess silicon compared to the $FeSi_2$ stoichiometry. We have therefore performed a set of irradiations at 550 °C, to 1×10^{16} ions/cm^2, with different Xe energies. The component depth profiles, derived from the RBS analysis of the samples implanted at 150, 250, 475, and 700 keV Xe, are shown in Fig. 8(a). In all cases we found complete intermixing, i.e., silicon diffusing to the surface, though the components had different depth distributions. In the sample implanted with 150 keV, the Fe and Si profiles are not as homogeneous in the surface region as for 250 keV, and Xe is distributed deeper into the silicon substrate, and, accordingly, the Fe profiles have longer distribution tails in the silicon substrate. Via CEMS we determined the β-$FeSi_2$ fraction as a function of the irradiation energy, plotted in Fig. 8(b). The curve shows an increased growth of β-$FeSi_2$, with a saturation around 60%. However, although we have a higher yield of β-$FeSi_2$, the deep Fe distribution tials were not desirable, and the high implantation energies were not used in further experiments.

4. Full growth of β-FeSi₂

Complete growth of the β-$FeSi_2$ phase by ion beam mixing of 35 nm Fe/Si bilayers was achieved at a Xe ion energy of 205 keV, a fluence of 2×10^{16} ions/cm^2, and a target temperature of 600 °C. The results of RBS and CEMS analyses for this sample are summarized in Fig. 9. The concentration ratio of the components corresponds to that of stoichiometric $FeSi_2$. The calculated effective thickness of the layer is

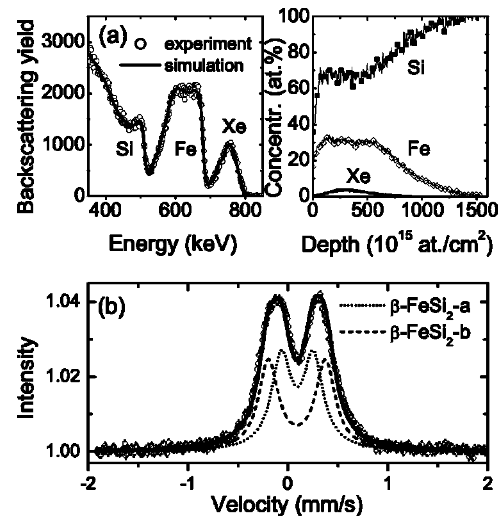

FIG. 9. RBS (a) and CEMS (b) analyses of 35 nm Fe/Si sample, implanted with 205 keV Xe, to 2×10^{16} ions/cm^2 at 600 °C, indicating a full growth of the β-$FeSi_2$.

[This article is copyrighted as indicated in the article. Reuse of AIP content is subject to the terms at: http://scitation.aip.org/termsconditions. Downloaded to] IP: 131.227.68.227 On: Wed, 30 Apr 2014 17:13:22

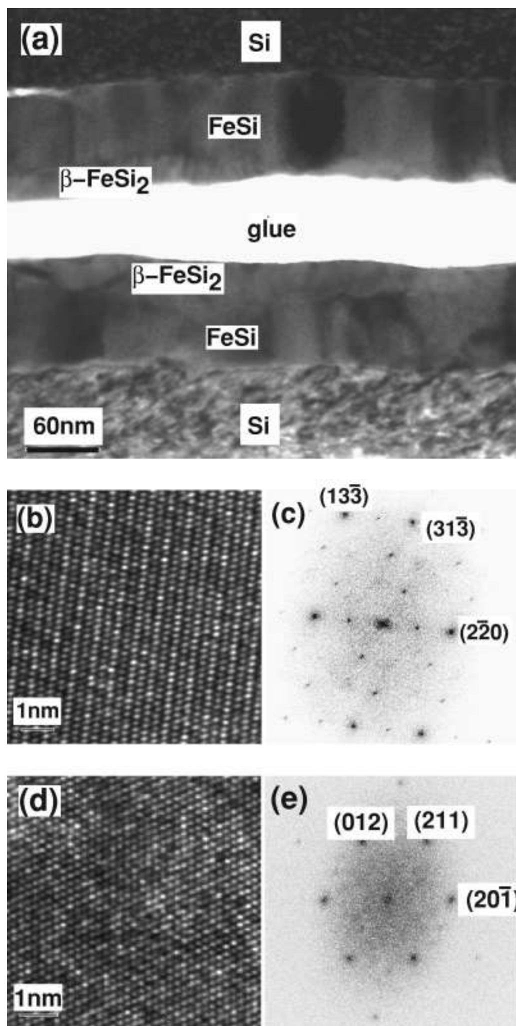

FIG. 10. TEM analysis of 35 nm Fe/Si, implanted with 250 keV Xe, to 2×10^{16} Xe ions/cm^2 at 400 °C: (a) low-magnification dark field micrograph showing the subdivision in a bottom and top silicide layer; (b) lattice image obtained in the top layer; (c) Fourier transform of the top layer lattice image; (d) lattice image obtained in the bottom layer; and (e) Fourier transform of the bottom layer lattice image, showing reflections corresponding to {001}, {221}, and {210} planes of FeSi.

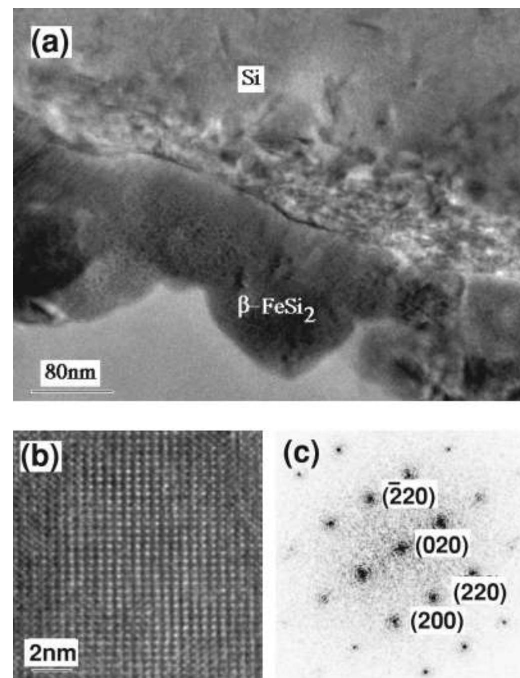

FIG. 11. TEM analysis of 35 nm Fe/Si, implanted with 250 keV Xe, to 2×10^{16} ions/cm^2 at 600 °C; (a) low-magnification birght field image showing a β-FeSi$_2$ layer on top of silicon; (b) lattice image from a thin area of the film; and (c) Fourier transform of the lattice image.

105(3) nm, and we still have a broad interface and surface roughness of 40(3) nm. The XRD analysis gives a spectrum similar to those shown for samples irradiated to the same fluence with 250 keV Xe at 550 and 600 °C. On the other hand, the CEMS spectrum can be fitted well with the doublets corresponding to a 100% pure β-FeSi$_2$ phase. Hence the full formation of this phase could be confirmed only by the more sensitive CEMS analysis.

C. Microstructural analysis

Cross-sectional TEM analyses were carried out for samples with partially or fully grown β-FeSi$_2$. In Fig. 10 we present the analysis of a 35 nm Fe/Si bilayer implanted at 400 °C with 250 keV Xe, to 2×10^{16} ions/cm^2. The RBS analysis of this sample showed a uniform depth distribution of Fe and Si in the inner parts of the silicide and an increased yield of silicon at the surface [see Fig. 4(d)], while CEMS indicated the presence of 38(4)% of β-FeSi$_2$. The low-magnification dark field micrograph, Fig. 10(a), shows a polycrystalline silicide layer, with a flat surface and a sharp interface with the silicon substrate. The crystal grains form a columnar structure, with the lateral size comparable to the layer thickness (~83 nm). Closer analysis reveals that the silicide has a double-layered structure. The top layer, which is labeled as β-FeSi$_2$ in regions where it can easily be distinguished from the bottom layer by diffraction contrast, makes up approximately 20% of the total film thickness. From high resolution TEM images and their Fourier transforms as well as EDXS analysis it follows that this layer consists of β-FeSi$_2$. As an example, Figs. 10(b) and 10(c) show a lattice image taken along the [334] zone axis of β-FeSi$_2$ and its Fourier transform, respectively. The Fourier transform shows reflections corresponding to {220}, {313}, and {133} planes of β-FeSi$_2$. The diffraction data in some cases show reflections that are forbidden in bulk β-FeSi$_2$, indicating a substantial amount of disorder in the top silicide. The corresponding analysis of the bottom layer gives two important results: crystallographic data are fully consistent with FeSi, (d) and (e), while EDX spectra yield Fe and Si concentrations of about 45 and 54 at. %, respectively. These data do not add up to 100% because of a small amount of Xe in the film. Also, the EDXS scanned laterally, showed constant Fe and Si concentrations within the bottom layer. Hence we may conclude that the bottom layer consists of Si-rich FeSi. The Si substrate preserves the single crystal structure, but there is a large amount of radiation damage. Note that the CEMS measurements probably overestimate the content of the β-FeSi$_2$ phase in this sample, which we attribute to interdiffused Si within the FeSi phase.

[This article is copyrighted as indicated in the article. Reuse of AIP content is subject to the terms at: http://scitation.aip.org/termsconditions. Downloaded to] IP: 131.227.68.227 On: Wed, 30 Apr 2014 17:13:22

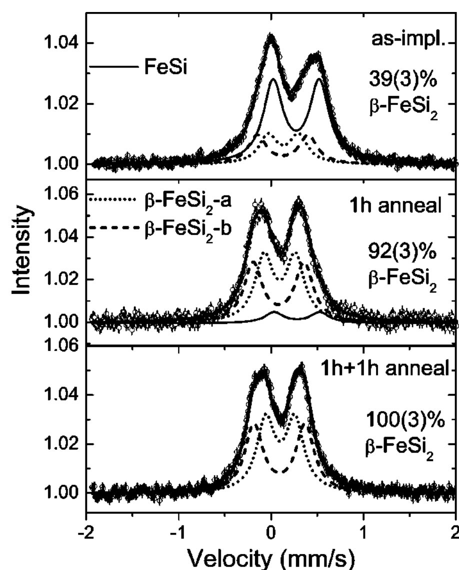

FIG. 12. CEMS analysis of: (a) as-implanted 35 nm Fe/Si, with 250 keV Xe, to 2×10^{16} Xe ions/cm^2 at 450 °C; (b) after 1 h annealing at 600 °C; and (c) after 1+1 h annealing at 600 °C.

The TEM analysis of the sample implanted at 600 °C with 205 keV Xe, to 2×10^{16} ions/cm^2, is shown in Fig. 11. In this case the silicide layer consists only of the polycrystalline β-FeSi$_2$ phase, which is concluded from crystallographic data obtained from electron diffraction and from Fourier transforms of the lattice images, Figs. 11(b) and 11(c). The Fourier transform shows reflections corresponding to (200), (020), (220), and (−220) planes of β-FeSi$_2$. In Fig. 11(a) it can be seen that the β-FeSi$_2$ crystal grains are not uniform in size and distribution. This micrograph, taken at lower magnification reveals that the silicide/Si interface is relatively sharp, but the surface of the silicide layer has a rather rough topography. This reflects in a nonhomogeneous silicide/silicon interface observed by RBS. The (111)Si/(020)β-FeSi$_2$ epitaxial crystallographic orientation starts from the Si substrate and holds throughout the grown grains. However, there are some differently oriented β-FeSi$_2$ grains at the surface. The lateral dimensions of the crystal grains range from 50 to 150 nm. Because of the shape and size of the grains, here we can only consider an effective thickness of the β-FeSi$_2$ layer of ~105 nm, as obtained from RBS. Residual radiation damage in silicon is lower than in the sample shown previously. This results from a higher target temperature during irradiation, at which silicon from the damaged zone is consumed in the Fe–Si reaction.

D. Growth of β-FeSi$_2$ by additional annealing

Complete formation of β-FeSi$_2$ was also achieved by additional vacuum annealing of ion-mixed samples. In Figs. 12 and 13 we present the results of CEMS and RBS analyses of a 35 nm Fe/Si sample irradiated with 250 keV Xe, to 2×10^{16} ions/cm^2 at 450 °C, and consequently annealed for 1+1 h at 600 °C. The as-implanted sample contains 39(3)% β-FeSi$_2$ and 61(3)% FeSi, but transforms to pure β-FeSi$_2$ after annealing for 2 h. After only 1 h of annealing there was still a 8(3)% fraction of FeSi in the sample. This could not be

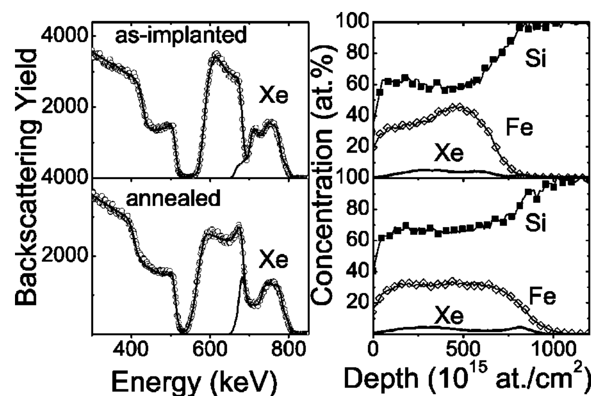

FIG. 13. RBS analysis of as-implanted 35 nm Fe/Si, with 250 keV Xe, to 2×10^{16} Xe ions/cm^2 at 450 °C, and after 1 h annealing at 600 °C.

resolved in the RBS spectra, which were practically identical after each of the two annealings and gave a Fe/Si ratio corresponding to FeSi$_2$. In the surface region of the as-implanted sample we observed the FeSi$_2$ stoichiometry. Similar to the sample irradiated at 400 °C, we presume that here we have a β-FeSi$_2$ nucleation front, which is more progressed at the irradiation temperature of 450 °C. By analogy, the inner part of the silicide layer consists of a Si-rich FeSi phase. The first hour of annealing induced additional Si diffusion to achieve the FeSi$_2$ stoichiometry, and the second annealing enabled a full transformation from FeSi to β-FeSi$_2$. The effective thickness of the grown β-FeSi$_2$ layer is 105(3) nm, and the interface and surface width 24(3) nm, much sharper compared to the samples where this phase was grown by direct ion-beam mixing. In the as-implanted sample, Xe has a double-peak distribution, with the first maximum located at 42(3) nm and the second at 72(3) nm. After annealing we observe a partial redistribution of the implanted Xe. The first maximum remains at the same position but with a slightly lower Xe concentration, and the second maximum moves to the silicide/silicon interface, at 102(3) nm. The XRD analysis of the as-implanted sample is seen from Fig. 6(b). After the first annealing there is an increased intensity of characteristic reflections from (220)/(202) and (422) β-FeSi$_2$, which are approximately equal in height, and after the second annealing there is an increased yield from (220)/(202) compared to (422) β-FeSi$_2$, as in the other cases when we are approach full growth of this phase.

IV. DISCUSSION

Studies of thermally induced solid-state reactions between thin Fe films and Si substrates indicated that β-FeSi$_2$ grows in a two-step process, starting with the formation of FeSi which then transforms to FeSi$_2$.[8] Silicon is the diffusion species in this system. This means that single-phase β-FeSi$_2$ can be grown in a thin film reaction when there is a limited supply of Fe and an unlimited supply of silicon. The measured[7,8] activation energies for the formation of FeSi are 1.67(15) eV on (100) Si and 1.36(25) eV on (111) Si, and 2.6(5) eV for β-FeSi$_2$. As reported by Lau *et al.*,[7] complete transformation of ~100 nm Fe on Si into FeSi was achieved by annealing for about 30 min at 500 °C; at 550 °C the

[This article is copyrighted as indicated in the article. Reuse of AIP content is subject to the terms at: http://scitation.aip.org/termsconditions. Downloaded to] IP: 131.227.68.227 On: Wed, 30 Apr 2014 17:13:22

β-$FeSi_2$ phase starts to nucleate. Radermacher *et al.*[8] achieved full growth of FeSi by rapid thermal annealing, for up to 60 s at 600 °C, while nucleation of β-$FeSi_2$ was registered for processing temperatures above 675 °C. Formation of FeSi is a diffusion-controlled process, and the silicide grows layer by layer. The β-$FeSi_2$ phase starts to nucleate at isolated sites, such as grain boundaries in the FeSi layer or stress-induced "weak" spots at the silicide/silicon interface.[37] This reaction, being nucleation-controlled, builds up β-$FeSi_2$ in the form of islands or columnar patches throughout the FeSi layer. For this reason the RBS profiles cannot distinguish between the two phases, but rather indicate various stages of phase transformation, similar to that in samples where growth of β-$FeSi_2$ is not completed. In the case of Fe ion implantation into Si at 300–350 °C, β-$FeSi_2$ precipitates are formed under the extreme nonequilibrium conditions, in a supersaturated silicon-rich environment.[4,8] For low Fe fluences the first $FeSi_2$ precipitates that nucleate are γ and α, while β-$FeSi_2$ predominates when the Fe/Si concentration ratio reaches the value of 1/2.[38] A similar, silicon-rich environment is present in IBIEC of Si preimplanted with Fe. Here the α precipitates were found to be understoichiometric, and both γ and α were metastable with respect to β-$FeSi_2$, with increasing the Fe concentration, or upon thermal annealing.[15,16]

In the experiments presented here the influence of both thermal and ion irradiation effects is important. The effects of ion irradiation are clearly seen at temperatures below 450 °C. Indeed, already after irradiation at 300 °C, a fully intermixed matrix is formed which contains 31(4)% $FeSi_3$, 35(4)% FeSi, and 34(4)% β-$FeSi_2$. Note that a thermal treatment would not yield the latter two phases. This difference is assigned to the high density of defects introduced during ion-beam bombardment, in collision cascades and thermal spikes combined with radiation enhanced diffusion and chemical driving forces, as described, e.g., by Bolse.[39] The nonequilibrium ballistic and thermal spike processes provide sufficient local energy transfer for nucleation and growth of β-$FeSi_2$. The energy deposited in the intermixed region by the impact ions is up to 4 keV/nm in the case of Xe. As compared to only thermal treatments, in the dynamic process of ion-beam mixing there are numerous atomic movements and displacements, amorphization, and recrystallization taking place simultaneously. Therefore crystal grains, grain boundaries, or nucleation sites cannot be considered the same as in thermal diffusion. By analogy to ion-beam synthesis, or IBIEC, a supersaturated Si-rich environment is expected to be located at the silicide/silicon interface, from where the nucleation front of β-$FeSi_2$ should be predominant. However, in 35 nm Fe/Si implanted with 2×10^{16} Xe ions/cm^2 at 400 °C we have observed the growth of β-$FeSi_2$ grains starting from the surface. The inner part of the silicide layer consists of the Si-rich FeSi phase. Hence, contrary to random nucleation of β-$FeSi_2$ from FeSi found in thermal growth, ion-beam mixing induces a layer by layer growth, with the nucleation front starting from the surface. The supply of silicon for the reaction is provided by its rapid diffusion from the substrate during ion irradiation. Also, contrary to ion-beam synthesis or IBIEC the Fe-silicidation process is not taking place in a Si-rich environment, but rather in a Fe-rich environment, with interdiffused silicon in the Fe layer. With these conditions, we do not observe nucleation of metastable γ or α-$FeSi_2$ precipitates, but formation of stable FeSi and β-$FeSi_2$ phases. Similar depth profiles of Fe and Si were found in the sample implanted at 450 °C. A further increase of the Xe fluence at 400–450 °C would probably result in a more progressed nucleation front, i.e., in a higher fraction of the grown β-$FeSi_2$ phase. In the case of 50 nm Fe/Si we did only a few irradiations at 450 °C, where the ion fluence was probably too low to form a β-$FeSi_2$ nucleation front. More detailed work on ion-beam mixing in Fe/Si bilayers at lower temperatures is in progress.[40]

In the temperature range from 450 to 500 °C a strong influence of thermal growth of FeSi is visible. The target temperature is still not sufficient for purely thermal nucleation of β-$FeSi_2$, but additional energy is provided by the implanted ions. A rather high β-$FeSi_2$ fraction of 81(3)% is achieved by irradiation of 35 nm Fe/Si with 250 keV Xe at 500 °C to the fluence of 2×10^{16} ions/cm^2. Starting from this temperature, the Xe distribution has a single maximum located at about half-depth of the silicide layer, suggesting that in the initial stage of irradiation there is rapid growth of FeSi, and its sequential transformation to β-$FeSi_2$.

At the target temperature of 550–600 °C thermal nucleation of β-$FeSi_2$ starts, though the reaction is strongly enhanced by ion irradiation. After irradiation of 35 nm Fe/Si with 250 keV Xe to (1 to 2)$\times10^{16}$ ions/cm^2 we reach a component ratio that corresponds to $FeSi_2$, but there still remains a small FeSi fraction even in the samples in which the silicon concentration is higher than needed for disilicide formation. Single-phase growth of β-$FeSi_2$ was achieved by reducing the energy to 205 keV, i.e., by moving the maximum of the Xe distribution closer to the critical region where the remaining FeSi was located. This implies that, among the other ion-beam effects, rearrangement of chemical bonds is crucial to finalize the reaction. RBS and TEM analyses proved a rather nonuniform structure of the grown β-$FeSi_2$ layers, with a high degree of surface roughness. Such a structure can be assigned to the nonequilibrium nature of ion-beam mixing, and also to the nature of nucleation and growth of this phase. As described by Dimitriadis and Werner[38] and the references therein, in thermal treatments FeSi transforms to β-$FeSi_2$ in an exothermic reaction, and the growth of β-$FeSi_2$ can be explained by analogy to explosive crystallization. After spontaneous nucleation, the β-$FeSi_2$ phase grows rapidly, dissipating energy to the surrounding environment, which induces surface roughness. A further contribution for developing a rough topography comes from the change in local density, the growing β-$FeSi_2$ grains consuming silicon from the surrounding region. For comparison, from an Fe layer of thickness d the resulting β-$FeSi_2$ layer has a thickness of $3.2\times d$, and consumes a thickness of $3.4\times d$ of silicon. In the samples irradiated at 550–600 °C we could not determine a propagation of β-$FeSi_2$ nucleation front, but the samples exhibited an evident rapid diffusion of silicon to the surface. We presume that in this case nucleation of β-$FeSi_2$ starts randomly, induced both by thermal and ion

[This article is copyrighted as indicated in the article. Reuse of AIP content is subject to the terms at: http://scitation.aip.org/termsconditions. Downloaded to] IP: 131.227.68.227 On: Wed, 30 Apr 2014 17:13:22

irradiation effects. In the surface region silicon is supplied from the surrounding and is readily consumed by the growing β-$FeSi_2$ grains. At the silicide/Si interface silicon is supplied from the substrate. However, while there is an unlimited resource of silicon from the substrate, its quantity at the surface is limited. Consequently, the grown layer consists of β-$FeSi_2$ grains, which are nonuniform in size and shape, with a relatively sharp interface towards the Si substrate and pronounced surface roughness. Annealing of 35 nm Fe/Si samples previously implanted at 450 °C with 250 keV Xe, to 2×10^{16} ions/cm^2, yielded a smoother β-$FeSi_2$ layer. Here, after ion irradiation, we had a β-$FeSi_2$ phase with a smooth surface at the top, and a Si-rich FeSi towards the substrate. Thermal treatment has enabled a supply of silicon from the substrate and a gradual phase transformation in the inner layer. Full transformation to the β-$FeSi_2$ layer was achieved at a moderate temperature of 600 °C. The role of premixing could be in eliminating the effects of residual impurities at the original Fe/Si interface, and hence allowing a direct influence of the Si substrate on the silicidation process.[41]

V. CONCLUSIONS

In this article, we presented a detailed study of the formation of β-$FeSi_2$ layers by ion-beam mixing of Fe/Si bilayers with noble-gas ions. The primary objective was to optimize the parameters in view to achieve growth of single-phase β-$FeSi_2$, to characterize the microstructure, and to qualitatively understand the importance of thermal and ion-induced energy deposition. It was demonstrated that ion-beam mixing can be used successfully for low temperature growth of β-$FeSi_2$, either directly or combined with postirradiation annealing. As to the temperature dependence of the process, we found that ion irradiation induces nucleation and growth of this phase at 300–400 °C, significantly lower than required even for the formation of the low temperature FeSi phase. Especially in samples irradiated at 400–450 °C, a layer-by-layer growth of β-$FeSi_2$, starting from the surface, was found. The impact ion induces a rapid diffusion of silicon to the surface and deposit sufficient energy to initiate nucleation in this region. This growth mechanism is apparently different from that in solid phase epitaxy, where β-$FeSi_2$ nucleates randomly in a FeSi matrix. At 500–600 °C there is a significant contribution of thermally activated growth of Fe-silicides. A full transformation of 35 nm Fe on Si to a 105 nm β-$FeSi_2$ layer was achieved by irradiation with 205 keV Xe to 2×10^{16} ions/cm^2, at 600 °C. The required temperature is substantially lower than that applied in other methods of preparation. The grown layer consists of epitaxial grains with a preferred (111)Si/$(020)\beta$-$FeSi_2$ crystallographic orientation. The grains are irregular in shape and size, which reflects in a pronounced surface roughness. We propose that this structure results from the growth of β-$FeSi_2$ grains in a local surrounding of interdiffused silicon. Smoother β-$FeSi_2$ layers are obtained when post-annealing previously intermixed Fe/Si at a moderate temperature of 600 °C.

ACKNOWLEDGMENTS

The authors are indebted to Professor G. Principi, Padova, for the help with some of the CEMS measurements and to Professor J. Keinonen and T. Sajavaara, Helsinki, for their cooperation on the ERDA analysis. This work has been funded by BMBF.

[1] D. Leong, M. Harry, K. J. Reeson, and K. P. Homewood, Nature (London) **387**, 686 (1997).
[2] M. C. Bost and J. E. Mahan, J. Appl. Phys. **58**, 2696 (1985).
[3] Z. Yang, K. P. Homewood, M. S. Finney, M. A. Harry, and K. J. Reeson, J. Appl. Phys. **78**, 1958 (1995).
[4] H. Katsumata, Y. Makita, N. Kobayashi, H. Shibata, M. Hasegawa, I. Aksenov, S. Kimura, A. Obara, and S. Uekusa, J. Appl. Phys. **80**, 5955 (1996).
[5] S. Brehme, P. Lengsfeld, P. Strauss, H. Lange, and W. Fuhs, J. Appl. Phys. **84**, 3187 (1998).
[6] Y. Makita, Future generation photovoltaic technologies: first NREL Conference, The American Institute of Physics 1-56396-704-9/97, 3 (1997).
[7] S. S. Lau, J. S.-Y. Peng, J. O. Olowolafe, and M.-A. Nicolet, Thin Solid Films **25**, 423 (1975).
[8] K. Radermacher, S. Mantl, Ch. Dieker, H. Lüth, and C. Freiburg, Thin Solid Films **215**, 76 (1992).
[9] D. Mangelinck, L. Wang, C. Lin, P. Gas, J. Grahn, and M. Ostling, J. Appl. Phys. **83**, 4193 (1998).
[10] L. T. Vinh, J. Chevrier, and J. Derrien, Phys. Rev. B **46**, 15946 (1992).
[11] A. Terrasi, S. Ravesi, M. G. Grimaldi, and C. Spinella, J. Vac. Sci. Technol. A **12**, 289 (1994).
[12] T. Yoshitake, T. Nagamoto, and K. Nagayama, Thin Solid Films **381**, 236 (2001).
[13] H. C. Cheng, T. R. Yew, and L. J. Chen, Appl. Phys. Lett. **47**, 128 (1985).
[14] L. Wang, C. Lin, Q. Shen, X. Lin, R. Ni, and S. Zou, Appl. Phys. Lett. **66**, 3453 (1995).
[15] J. Desimoni, F. H. Sanchez, M. B. Fernandez van Raap, X. W. Lin, H. Bernas, and C. Clerc, Phys. Rev. B **54**, 12787 (1996).
[16] M. Behar, H. Bernas, J. Desimoni, X. W. Lin, and R. L. Maltez, J. Appl. Phys. **79**, 752 (1996).
[17] S. B. Ogale, R. Joshee, V. P. Godbole, S. M. Kanetkar, and V. G. Bhide, J. Appl. Phys. **57**, 2915 (1985).
[18] D. M. Phase, V. P. Godbole, V. N. Kulkarni, S. B. Ogale, and V. G. Bhide, Nucl. Instrum. Methods Phys. Res. B **19/20**, 737 (1987).
[19] D. L. Santos, J. P. de Souza, L. Amaral, and H. Boudinov, Nucl. Instrum. Methods Phys. Res. B **103**, 56 (1995).
[20] M. Milosavljevic, S. Dhar, P. Schaaf, N. Han, and K.-P. Leib, Appl. Phys. A: Mater. Sci. Process. **71**, 43 (2000); Nucl. Instrum. Methods Phys. Res. B **178**, 229–232 (2001).
[21] A. Dobrosavljević, M. Milosavljević, N. Bibić, and A. Efremov, Rev. Sci. Instrum. **71**, 786 (2000).
[22] K.-P. Lieb, Contemp. Phys. **40**, 385 (1999).
[23] M. Uhrmacher, K. Pampus, F. J. Bergmeister, D. Purschke, and K.-P. Lieb, Nucl. Instrum. Methods Phys. Res. B **9**, 234 (1995).
[24] L. R. Doolittle, Nucl. Instrum. Methods Phys. Res. B **9**, 344 (1985).
[25] P. Schaaf, A. Krämer, l. Blaes, G. Wagner, F. Aubertin, and U. Gonser, Nucl. Instrum. Methods Phys. Res. B **53**, 184 (1991).
[26] F. Landry and P. Schaaf (unpublished).
[27] J. Jokinen, J. Keinonen, P. Tikkanen, A. Kuronen, T. Ahlgren, and K. Nordlung, Nucl. Instrum. Methods Phys. Res. B **119**, 533 (1996).
[28] M. Fanciulli, C. Rosenbald, G. Weyer, S. Svane, and N. E. Christensen, Phys. Rev. Lett. **75**, 1642 (1995).
[29] M. Fanciulli, C. Rosenblad, G. Weyer, A. Svane, N. E. Christensen, H. von Känel, and C. O. Rodriguez, J. Phys.: Condens. Matter **9**, 1619 (1997).
[30] J. Desimoni and F. H. Sanchez, Hyperfine Interact. **122**, 277 (1999).
[31] K. Vojtyzechovsky and T. Zemcik, Czech. J. Phys., Sect. B **24**, 171 (1974).
[32] R. Wandji, C. LeCorre, J. M. R. Genin, and B. Roques, Phys. Status Solidi B **45**, K123 (1971).
[33] H. Reuther, M. Dobler, G. Behr, and J. Schumann, Hyperfine Interact. C **3**, 385 (1998).

[This article is copyrighted as indicated in the article. Reuse of AIP content is subject to the terms at: http://scitation.aip.org/termsconditions. Downloaded to] IP: 131.227.68.227 On: Wed, 30 Apr 2014 17:13:22

[34] G. K. Wertheim, J. H. Wernick, and D. N. E. Buchanan, J. Appl. Phys. **37**, 3333 (1996).
[35] O. Helgason and T. I. Sigfusson, Hyperfine Interact. **45**, 415 (1989).
[36] J. F. Ziegler, J. P. Biersack, and U. Littmark, *The Stopping and Range of Ions in Solids* (Pergamon, New York, 1985); PC program package TRIM95 (1995).
[37] C. A. Dimitriadis and J. H. Werner, J. Appl. Phys. **68**, 93 (1990).
[38] M. Dobler, H. Reuther, M. Betzl, M. Mäder, and W. Möller, Nucl. Instrum. Methods Phys. Res. B **117**, 117 (1996).
[39] W. Bolse, Mater. Sci. Eng., R. **12**, 53 (1994).
[40] N. Bibić, S. Dhar, M. Milosavljević, P. Schaaf, and K. P. Lieb (unpublished).
[41] M. Milosavljević, N. Bibić, D. Peruško, C. Jeynes, and U. Bangert, Solid State Phenom. **71**, 147 (2000).

[This article is copyrighted as indicated in the article. Reuse of AIP content is subject to the terms at: http://scitation.aip.org/termsconditions. Downloaded to] IP: 131.227.68.227 On: Wed, 30 Apr 2014 17:13:22